Alexander Thiesen*, Sylvia Pfensig, Wolfram Schmidt, Frank Kamke, Jörg Kaminsky, Stefan Siewert, and Klaus-Peter Schmitz

Development of a Low-Cost Electrodynamic Fatigue Testing System with Automated Sine Wave Quality Assessment

https://doi.org/10.1515/cdbme-2025-0177

Abstract: Dynamic fatigue testing of medical devices represents a complex and expensive process. Universal electrodynamic testing machines are costly. Price scales with the number of devices under test. For accurate testing, the machine must produce the specified conditions. This includes amplitude and frequency but also the loading curve shape. While continuous tracking of amplitude and frequency has become standard practice, current methodologies still rely on optical and intermittent observations for analyzing the curve shape. In this study, we present a solution that combines cost-effective electrodynamic fatigue testing devices with a custom feedback control system. The system uses a windowed discrete Fourier transform with peak finding to determine the relevant parameters. The proposed system has been deployed in two test setups. A transfer to further test applications can easily be implemented.

Keywords: Dynamic Testing, Fatigue Testing, Implant and Material Testing, Electrodynamic Testing Machine, Feedback Control System, Real-Time Measurement, Discrete Fourier Transform, Sine Wave Quality Assessment

1 Introduction

Dynamic fatigue testing represents a critical aspect in evaluating the durability and reliability of medical devices, where precise control of load and deformation is essential. We are working with products whose testing has to comply with ISO 25539-2 and ASTM F2477 [2, 5].

Traditionally dynamic fatigue testing systems only evaluate amplitude and frequency and give a visual view of the curve shape. In cases of slow or unexpected curve shape deformation, which can occur due to changes in the environment

*Corresponding author: Alexander Thiesen, Institut für ImplantatTechnologie und Biomaterialien e.V.,

Friedrich-Barnewitz-Straße 4, 18119 Rostock-Warnemünde, Germany, e-mail: alexander.thiesen@iib-ev.de

Sylvia Pfensig, Wolfram Schmidt, Frank Kamke, Jörg Kaminsky, Stefan Siewert, Klaus-Peter Schmitz, Institut für Implantat-Technologie und Biomaterialien e.V., Friedrich-Barnewitz-Straße 4, 18119 Rostock-Warnemünde, Germany

of the test setup, these control systems are not able to react to these changes.

Our system introduces an automated sine wave quality assessment, which provides both automatic response and user feedback. Our system uses electrodynamic pistons with an amplifier to generate the deformation or pressure. These systems are cost-effective compared to universal dynamic testing solutions offered by established suppliers. We developed a custom feedback control mechanism using discrete Fourier transformation performed on a microcontroller. This paper introduces the essential technical functions of the software and hardware components.

2 Application

The test setup described can be applied to various medical devices that require fatigue testing. Various mounting fixtures (e.g., clamp adapters, custom jigs) and force-transmission components allow for quick adaptation to different geometries and load paths. Typical applications include the creation of pulsatile heart blood pressure for testing of coronary stents and dynamic testing of fixation elements of devices in the heart or other positions with regular movement. Test frequency, amplitude, pre-load and fatigue mechanisms can be customized depending on the material properties and expected device lifetime.

3 Methods

The fatigue testing system consists of multiple separate functions. These functions require different hard- and software components. The following chapters discuss these functions and requirements. The functions of the system include:

- real-time data acquisition,
- short-cycle data evaluation and system control,
- data transfer,
- long-term data storage and a
- user interface.

3.1 Real-Time Evaluation

For real-time data acquisition and short-cycle data evaluation, an ESP32 microcontroller with a dual-core processor and 8 MB data storage was used. The dual-core processor allows independent real-time data acquisition on one core and short-cycle data evaluation on the other. Thus, one core continuously gathers accurately timed measurement data and performs real-time evaluation, while the other processes data packets that would cause unacceptable pauses if handled on a single core [4].

The measurement data is read digitally in serial from a laser distance sensor. However, any other input source directly correlated to the testing deformation, such as pressure, can be used. The real-time evaluation includes a total offset check to stop the system immediately if destructive conditions occur. The data is recorded in a circular buffer.

3.2 Short-Cycle Evaluation

The short-cycle evaluation is a packet-based data evaluation performed on the second core of the ESP32 microcontroller. The data is split into 1024 ms blocks. Each block is transformed into the frequency domain using a windowed discrete Fourier transform [6, 7, 8, 10].

For windowing, the SFT5M Flat-Top Window of Heinzel, Rüdiger, and Schilling [7] was chosen because it offers good amplitude accuracy with an acceptable trade-off in frequency resolution. The windowing function is displayed in Equation 1. With this function the shape of the window is calculated according to its size M with $z \in \{0, \ldots, M-1\}$ [1, 3, 7, 8].

$$\omega_j(z) = 0.209671 - 0.407331 \cdot \cos(1 \cdot z)$$

$$+0.281225 \cdot \cos(2 \cdot z) - 0.092669 \cdot \cos(3 \cdot z)$$

$$+0.0091036 \cdot \cos(4 \cdot z) \tag{1}$$

To obtain the amplitudes of the current frequencies, the frequency domain is condensed using a peak-finding algorithm. The algorithm defines a peak as a point that is higher than its two neighboring points, similar to the definition of a local maximum. Low noise peaks are filtered out. The amplitude is determined by adding the area under the peak over an interval around the maximum. If peaks are too close together, the areas around the peaks do not overlap but are separated by a midpoint between them. This method has been derived from O'Haver [9].

The condensed peaks are then divided into three groups: the static part around $0\,\mathrm{Hz}$, the dynamic part around the stimulus frequency, and the remaining frequencies. The sum of the remaining frequencies is used as a measure of the curve shape and sine wave quality. It is zero for a perfect sine wave.

3.3 Data Transfer

The evaluated data and test settings are transferred from the ESP32 microcontroller to a Raspberry Pi 5 running a Debian Linux system. The connection is established via USB in serial mode. A custom-developed data transfer protocol is implemented on both sides. It offers binary, packet-based transfer including packet identifiers, packet numbering, and content checks using a CRC32 checksum. Configuration packets and condensed measurement data are organized into Protocol Buffers. This ensures version compatibility and optimizes the development process. Complete measurement arrays are transferred as simple binary arrays.

On the Linux side, the data is processed using a Python program. This program runs the transfer protocol and manages the transfer of the settings and measurement data from the microcontroller to the databases.

3.4 Data Storage

The data is stored in two databases. Settings and condensed measurement data are saved in a time-based database. This ensures that the test is completely traceable and flexible. System conditions and a live view of the oscillation are stored in a simple NoSOL in-memory database.

3.5 User Interface

The user interface software does not need direct access to the microcontroller or the Linux-based control system. It only interacts with the databases described above. Settings and commands are written to the databases and executed by programs on the control system or transferred to the microcontroller. The measurement data is read from the same databases for display. In our solution, the user interface is written in PySide6 using Python.

4 Results and Discussion

The system has been evaluated by checking the accuracy of the data analysis on artificial data and optically on a running system. One machine has completed 20 million cycles in testing and is running 400 million cycles for further testing.

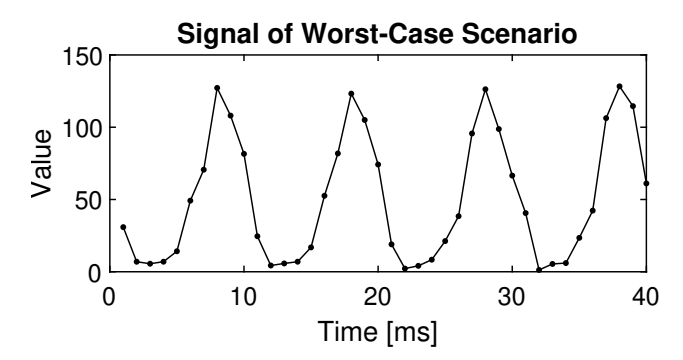


Fig. 1: Signal of a purposely created worst-case scenario. Negative values cannot be handled by the test setup and create disturbances in the curve shape near zero.

4.1 Measurement Evaluation

Preliminary tests of the analysis software were performed to evaluate the possible analysis setups. These tests led to the proposed test setup.

The tests were also performed on a purposely created worst-case scenario. This test setup used the specified maximum frequency and parameters that produced negative values that could not be handled by the system. The resulting signal in Figure 1 therefore shows a flat profile for values near zero and sharp peaks. A curve shape like this should be detected and reported as an error. This signal was windowed and transformed into the frequency domain. Figure 2 shows the result of this transformation. Due to the discrete transformation, the amplitudes leak into nearby frequencies, forming broader peaks. To determine the amplitudes of the frequencies, the leaked energy is summed into the corresponding core frequency bins. The results of this peak-finding can be seen in Figure 3. The peak at 0 Hz is used as the static offset, while the peak at the stimulus frequency 100 Hz represents the amplitude of the dynamic part. The sum of the other frequencies affects the curve shape and is therefore used as an indication of sine wave quality. In this example, the sum of these frequencies is higher than the amplitude at the stimulus frequency, indicating a highly disturbed curve shape.

4.2 Optical Evaluation

In addition to the processing evaluation using the measurements taken by the test setup, an independent measurement was performed and evaluated using an optical technique.

The movement of the test setup was recorded with the high-speed camera Os7 from Integrated Design Tools, Inc., California, USA. The image contained a moving element of the electrodynamic piston and a length reference. The laser measurement was taken close by. The optoNCDT2300

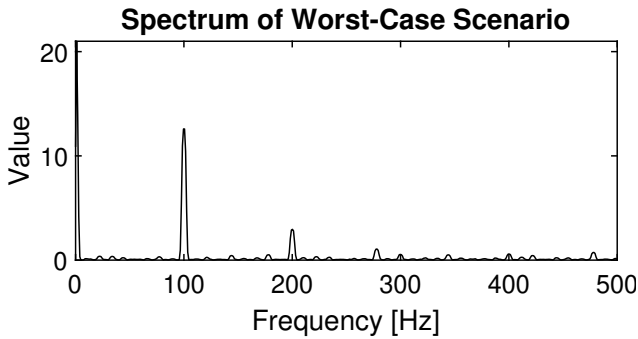


Fig. 2: Spectrum after discrete Fourier transformation of a purposely created worst-case scenario. Peaks leak into surrounding frequencies, resulting in broader peaks. The static offset appears near $0\,\mathrm{Hz}$ and the dynamic part near $100\,\mathrm{Hz}$. Smaller disturbance peaks are spread over the whole frequency range.

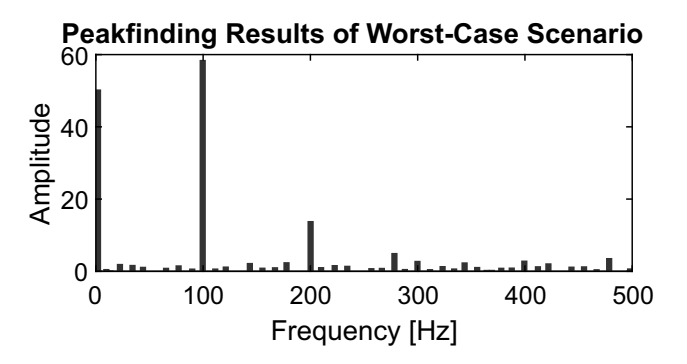


Fig. 3: Peak-finding results of the purposely created worst-case scenario. Leaked frequencies are summed to provide a simplified display of energy per frequency. The static offset appears near $0\,\mathrm{Hz}$ and the dynamic part near $100\,\mathrm{Hz}$, while smaller disturbance peaks are spread over the frequency range.

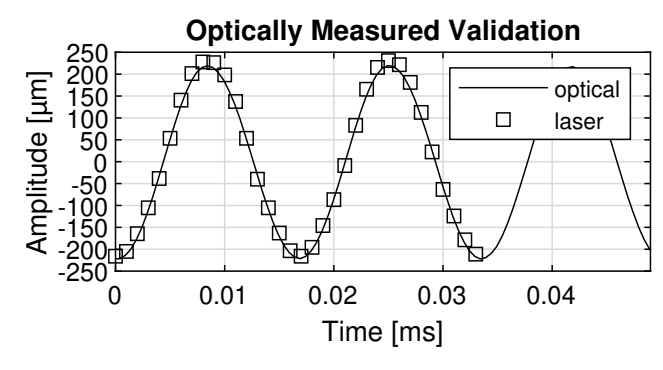


Fig. 4: Signal of running Test with a set Amplitude of $225\,\mu\mathrm{m}$ and a frequency of $60\,\mathrm{Hz}$. The signal is measured optically with a high-speed camera and with a laser in two graphs. Both measurements show different points in time. Laser measurements show a little higher amplitude of $5\,\mu\mathrm{m}$.

ILD2300-100 laser from Micro-Epsilon Messtechnik GmbH & Co. KG, Ortenburg, Germany, was used. It was calibrated to a maximal relative deviation of 0.78 %. The images were recorded with a sampling rate of 2000 Hz. After recording the video images were measured with the motion analysis software ProAnalyst from Xcitex Inc., Massachusetts, USA. 12 consecutive peaks where recorded.

With a set amplitude of $225 \, \mu m$ the optical measurements showed an amplitude of $220 \, \mu m$ The measurement resolution of the camera was $4.5 \, \mu m \, px^{-1}$. The standard deviation over the 12 peaks was $1.26 \, \mu m$.

This recording and a recording using the laser are compared in Figure 4. The laser shows a slightly higher amplitude of 223 µm compared to the high-speed camera for one period measured using the maximum and minimum.

The inaccuracies between the measurement systems are acceptable. No considerable differences between the analysis and the measurements could be found. This enables the test setup to be used for amplitudes in the micrometer and millimeter range.

5 Conclusion and Future Work

The results show that the implementation of the test system is successful. High precision in the movement was achieved, allowing tests with small and medium amplitudes ranging from micrometers to millimeters. This enables the construction of test setups for, stents and other small mechanical medical devices.

In the future, the test setup will undergo further intensive testing and error analysis. This integrated system architecture might be implemented in future dynamic fatigue testing setups.

Author Statement

Research Funding: The financial support by the European Regional Development Fund (ERDF) and the European Social Fund (ESF) within the collaborative research between economy and science of the state Mecklenburg-Vorpommern is gratefully acknowledged. Conflict of interest: The authors declare no conflict of interest.

References

- [1] Tilman Butz. "Fensterfunktionen." In: Fouriertransformation für Fußgänger. Ed. by Tilman Butz. 7., aktualisierte Auflage. Studium. Wiesbaden: Vieweg+Teubner, 2011, pp. 71–92. ISBN: 978-3-8348-0946-9. DOI: 10.1007/978-3-8348-8295-0_4.
- [2] Cardiovascular implants Endovascular devices. ISO 25539-2:2020. URL: https://www.iso.org/standard/69835. html (visited on 03/20/2025).
- [3] Gabriele D'Antona and Alessandro Ferrero. Digital signal processing for measurement systems. Theory and applications. Information technology. New York, NY: Springer, 2006. 267 pp. ISBN: 978-0-387-24966-7. DOI: 10.1007/0-387-28666-7.
- [4] Espressif Systems (Shanghai) Co., Ltd., ed. ESP32-WROVER-E & ESP32-WROVER-IE Datasheet. Version 2.0. 2024. URL: https://www.espressif.com/sites/default/files/documentation/esp32-wrover-e_esp32-wrover-ie_datasheet_en.pdf (visited on 03/20/2025).
- [5] F04 Committee, ed. Test Methods for in vitro Pulsatile Durability Testing of Vascular Stents and Endovascular Prostheses. ASTM F2477-24. West Conshohocken, PA: ASTM International, July 18, 2024. DOI: 10.1520/F2477-24. URL: https://store.astm.org/f2477-24.html (visited on 03/20/2025).
- [6] Claude Gasquet and Patrick Witomski. Fourier analysis and applications: filtering, numerical computation, wavelets. In collab. with R. Ryan. Vol. 30. Texts in applied mathematics 30. New York: Springer, 1999. ISBN: 0387984852.
- [7] G. Heinzel, A. Rüdiger, and R. Schilling. Spectrum and spectral density estimation by the Discrete Fourier transform (DFT), including a comprehensive list of window functions and some new at-top windows. 2002. URL: https: //pure.mpg.de/rest/items/item_152164/component/file_ 152163/content (visited on 04/04/2024).
- [8] André Neubauer. DFT Diskrete Fourier-Transformation. Wiesbaden: Vieweg+Teubner Verlag, 2012. ISBN: 978-3-8348-1996-3. DOI: 10.1007/978-3-8348-1997-0.
- [9] Tom O'Haver. Peak Finding and Measurement. Ed. by University of Maryland. 2022. URL: https://terpconnect.umd.edu/~toh/spectrum/PeakFindingandMeasurement.htm (visited on 02/13/2024).
- [10] Gerlind Plonka-Hoch et al. Numerical Fourier analysis. Applied and Numerical Harmonic Analysis. Cham: Birkhäuser, 2018. ISBN: 9783030043056. DOI: 10.1007/978-3-030-04306-3. URL: https://zbmath.org/?q=an:1412.65001.